frontiers | Frontiers in Earth Science

TYPE Original Research
PUBLISHED 06 March 2024
DOI 10.3389/feart.2024.1349195

Check for updates

OPEN ACCESS

EDITED BY
David K. Wright,
University of Oslo, Norway

REVIEWED BY
Junghyung Ryu,
Pukyong National University, Republic of Korea
Zhixiong Shen,
Coastal Carolina University, United States
Yuecong Li,
Hebei Normal University, China

*CORRESPONDENCE
Linjing Liu,
liulinjing@mail.cgs.gov.cn
Zhe Liu,
liuzhe@mail.cgs.gov.cn

RECEIVED 04 December 2023
ACCEPTED 19 February 2024
PUBLISHED 06 March 2024

CITATION
Yang J, Liu L, Roberts H, Liu Z, Song L and Zhang P (2024), Holocene flood records and human impacts implied from the pollen evidence in the Daming area, North China Plain.
Front. Earth Sci. 12:1349195.
doi: 10.3389/feart.2024.1349195

COPYRIGHT
© 2024 Yang, Liu, Roberts, Liu, Song and Zhang. This is an open-access article distributed under the terms of the Creative Commons Attribution License (CC BY). The use, distribution or reproduction in other forums is permitted, provided the original author(s) and the copyright owner(s) are credited and that the original publication in this journal is cited, in accordance with accepted academic practice. No use, distribution or reproduction is permitted which does not comply with these terms.

Holocene flood records and human impacts implied from the pollen evidence in the Daming area, North China Plain

Jinsong Yang[1], Linjing Liu[1]*, Harry Roberts[2], Zhe Liu[1]*, Lei Song[1] and Peng Zhang[3]

[1]Key Laboratory of Quaternary Chronology and Hydro-Environmental Evolution, Institute of Hydrogeology and Environmental Geology, China Geological Survey, Shijiazhuang, China, [2]Department of Past Landscape Dynamics, Institute of Geography and Spatial Organization, Polish Academy of Sciences, Warsaw, Poland, [3]Hebei Institute of Geological Survey, Shijiazhuang, Hebei, China

Understanding the environmental significance of pollen and spores in alluvial plains is important for stratigraphic correlation and paleoenvironmental reconstruction. This paper presents palynological data from the North China Plain and explores their relationship with paleoflood records and human impacts since the Holocene. Our data reveal that pollen concentration and pollen assemblage vary in flood deposits (including overbank deposits and slackwater deposits) and inter-flood deposits (including sandy soils and lacustrine deposits). Flood deposits have higher fern percentages (28.6%) and lower herbaceous percentages (14.8%) compared to inter-flood deposits, though slackwater deposits share similar pollen concentrations and assemblages with sandy soils. Notably, overbank deposits are characterized by pollen-poor zones and aggregation of deteriorated pollen grains, especially in Unit III (755–385 cm, ca. 3.2–2.2 ka) and Unit V (190–0 cm, after ca. 0.6 ka). These findings suggest that overbank deposits correspond to strengthened hydrodynamic conditions at the flood-peak stage. Furthermore, the indicative pollen and spores provide compelling evidence for intensifying human impact in the North China Plain since the late Holocene. An aggregation of *Selaginella sinensis* at the depth of 640–610 cm indicates deforestation in the uplands since ca. 2.9 ka. Similarly, a sharp increase in Malvaceae percentage at the depth of 285–215 supports historical records of initial cotton planting in the Tang Dynasty (ca. 1.4–1.1 ka). The study underscores the value of palynological analysis for reconstructing paleoenvironment and human-environment interactions, providing a robust framework for understanding landscape evolution in the North China Plain.

KEYWORDS

pollen analysis, human activity, paleoflood, Holocene, North China Plain

1 Introduction

Fossil pollen extracted from sediments is a well-established proxy of past vegetation changes. It has become one of the most ubiquitous and valuable methods for paleoclimate, paleoecology and paleoenvironment research, especially in lakes, wetlands and oceans (Xu et al., 2016; Chevalier et al., 2020). Unlike these stable depositional environments, few samples for

palynological work have come from alluvial plains. Recent studies, however, have suggested that pollen records preserved in floodplain deposits and paleosols can reconstruct past climate, environment and human activity (Brown et al., 2008; Alexandrovskiy et al., 2016; Ricker et al., 2019; Liu et al., 2020).

Extensive alluvial deposits in the North China Plain (NCP) contain a wealth of information about fluvial geomorphology, environment, climate, and ecology (Tong et al., 1983; Lv et al., 2022). Pollen and spores have been used as an important method in these alluvial sediments. Fan et al. (2009) reconstructed the paleovegetation and environmental evolution since 3.50 Ma BP. Li et al. (2016) uncovered Holocene climate trends based on pollen-spore assemblages. However, several factors, such as deforestation, irrigation, pollen sorting and sedimentary environment, have made the interpretation of palynological data complicated and distorted (Zhu et al., 2002; Kumar et al., 2019). For example, modern pollen study of alluvium in the NCP shows that pollen assemblages vary within geomorphic settings and sedimentary facies (Xu et al., 1996). In addition, the sources of pollen grains in alluvial plains are diverse (e.g., Solomon et al., 1982; Kumar et al., 2019). In the NCP, most of the arboreal pollen is derived from the upland mountains, whereas the non-arboreal pollen is mainly derived from the local plain (Xu et al., 1996; Pang et al., 2011). It is necessary to carefully consider the pollen source when reconstructing paleoclimate and paleovegetation, as pollen can be transported from upstream mountains and local areas by wind and river (Yang et al., 2019; 2021). Therefore, there remains a need for a better understanding of the environmental significance of pollen and spores in the NCP.

Alluvial plains are formed from sediment deposited by rivers on the adjacent flood basin, mainly through inundations, crevasse splays and avulsions (Lombardo, 2016; Wohl, 2021). The Yellow River in the NCP is the world's most sediment-laden river, and the sediments are, therefore, vulnerable to natural and human interference (Chen et al., 2012; Chen, 2019). Fluvial processes and human activities are the two main factors influencing the NCP, which can be traced from pollen records (Xu et al., 2010; Liu et al., 2013; 2020). Several studies have explored the potential of using pollen to identify the difference between flood and intermittent-flood periods. Xu et al. (2010) found that alluvium dominated by *Pinus* and *Selaginella* was deposited during a flood. Liu et al. (2013) and Liu et al. (2016) argued that percentages of arboreal pollen in paleoflood deposits were higher than those in paleosols. In addition, pollen and spores can also be used as an indicator of anthropogenic activity (Li et al., 2008; Ding et al., 2011). For instance, the percentage growth of *Selaginella sinensis* in floodplain deposits implies intensive human influence, such as deforestation in upriver mountains areas (Zhang et al., 2007; Pang et al., 2011; Liu et al., 2013). These prior studies have uncovered the importance of flood and human impacts on pollen assemblages. Relative to the vast extent of the floodplain and the complex history of man-land relationships in the NCP, however, pollen as an indirect proxy still requires further study.

This study presents pollen and spore data from the Daming area on the NCP with three main objectives: a) to elucidate pollen content and composition in different sedimentary facies; b) to compare the pollen assemblages with paleoflood reconstruction results; and c) to imply the history of human impacts from the palynological data by synthesizing regional work and historical documents.

2 Regional setting

The research region is located in the center of the NCP (32°N-40°N, 114°E–122°E). It is one of the largest alluvial plains in eastern Asia, based on deposits from the Yellow River, Huai River, Hai River, and their tributaries in history (Shi et al., 2014). In particular, the landscape of the NCP during the late Holocene is closely related to breaches and diversions of the Yellow River (Chen et al., 2012). According to historical data, the lower Yellow River is highly susceptible to perturbations and diversions, and many abandoned river courses have been left in the floodplain (Chen, 2019) (Figure 1A).

The Daming area, located at the junction of Hebei, Shandong and Henan provinces in China (Figure 1B), is one of the most frequent diversion areas of the lower Yellow River and has extensive flood records (Yang et al., 2023a). The most severe hydrological event occurred when ancient Daming was submerged in 1401 AD (ca. 0.6 ka) due to an extreme flood (Daming County Local Gazetteers Compilation Committee, 1994). Furthermore, archaeological work has confirmed that the flood deposits from this event are approximately 1–5 m below the surface in the Daming area (Bai et al., 2015).

Previous research in the study area improves the understanding of flood history and pollen interpretation. Several historical floods recorded in nearby stratigraphic profiles have been reported, including Dazhanglong (Storozum et al., 2018a), Anshang (Storozum et al., 2018b), Sanyangzhuang (Kidder et al., 2012) and Shilipu (Yu et al., 2020). In addition, sporo-pollen fossils in Dongping Lake proved that the lake was frequently disturbed by inundations of the Yellow River in the last century (Chen et al., 2013; Yu et al., 2021) (Figure 1B).

3 Materials and methods

3.1 Longwangmiao profile

The Longwangmiao (LWM) site, one 9-m representative sedimentary profile, is located on the site of a disused brick factory, 10 km southeast of Daming County (Figure 1B). The LWM profile has been sensitive to environmental change since the Holocene, as fluvial-lacustrine sediments were interbedded with sandy soils. Based on our prior studies in the profile (Yang et al., 2023a; b), the Holocene paleoflood periods have been reconstructed using analysis of sedimentary characteristics, grain size and chemical composition. Our stratigraphy and paleoflood results are consistent with historical documents and regional archaeological work.

3.2 Dating methods

Due to the scarcity of plant fossils, only one humus soil sample at the top of lacustrine deposits was submitted to the Xi'an Accelerator

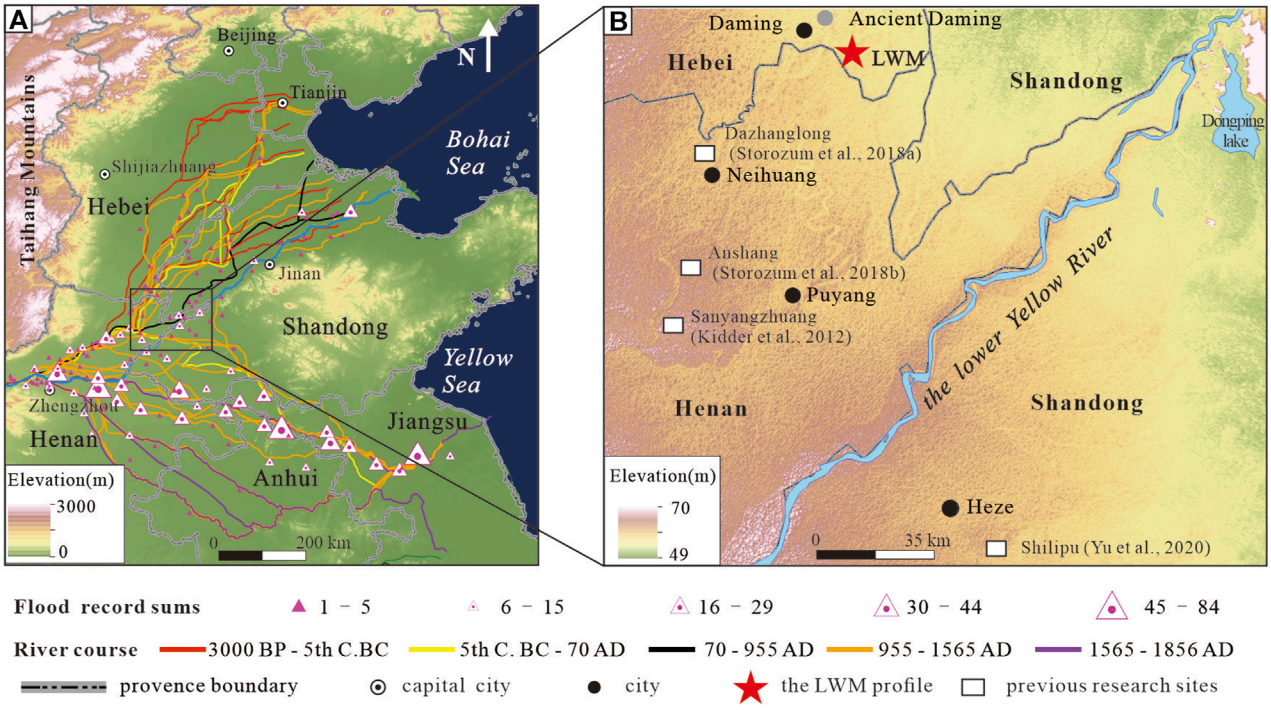

FIGURE 1
(A) The Yellow River course and flood record history in the North China Plain. **(B)** Location of the Longwangmiao (LWM) profile and previous research sites mentioned in this study. The flood records and river courses of the Yellow River refer from (Chen et al., 2012; Chen, 2019).

Mass Spectrometry Centre, China, for radiocarbon dating. The result is reported as radiocarbon ages as years before present with an analytical precision <0.5%. Calibration of age was carried out using the IntCal20 calibration curve (Reimer et al., 2020) and OxCal 4.4 (https://c14.arch.ox.ac.uk), which allows direct comparison with other ages.

Seven optically stimulated luminescence (OSL) samples, including six samples of flooding deposits and one sandy soil sample, were dated at the Key Laboratory of Quaternary Chronology and Hydro-Environmental Evolution, China Geological Survey. All of the samples were pretreated under the red light. The central parts of samples were treated with HCl (10%) and H_2O_2 (30%) to remove organic matter and carbonates. Coarse grains (63~90 μm and 90~125 μm) or fine grains (4~11 μm) were extracted based on particle size distribution of different samples (Table1). Then, the coarse grains were etched by HF (40%) for about 1 h, while the fine grains were treated with 30% fluorosilicic acid for about 5 days. The equivalent doses of the samples were measured by Lexsyg smart OSL/TL dating device. Single aliquot regenerative dose (SAR) protocol (Murray and Wintle, 2000; Wintle and Murray, 2006) was used. The U, Th and K concentrations were measured by Inductively Coupled Plasma Mass Spectrometry (ICP-MS) method. The water contents were estimated based on the values measured at laboratory and the sedimentary environments of the samples. The total dose rate was calculated by using the DRAC (Durcan et al., 2015). Based on all the radiocarbon dating and OSL results, the Bayesian age-depth model was established in R v.4.3.1, using package *bacon* v.2.3.9.1 (Blaauw et al., 2018).

3.3 Pollen and grain size analysis

Bulk samples for pollen and grain size analysis were obtained every 5 cm. 180 samples were conducted in the Key Laboratory of Quaternary Chronology and Hydro-Environmental Evolution, China Geological Survey. Pollen analysis followed using the conventional method (Faegri and Iversen, 1964). A tracer of modern Lycopodium spores with 27,637 ± 563 grains was added to each sample before chemical treatment. Pollen was counted under an Olympus BX51 microscope at ×400 magnification. Pollen taxonomy mainly followed Pollen Flora of China (Wang et al., 1995). The samples with a minimum of 100 grains were included in statistical analysis in accordance with the guide to the standardization of global palaeoecological data (Flantua et al., 2023) and related pollen research in nearby sites (Liu et al., 2013; Ren et al., 2019). In total, 97 out of 180 samples were counted for further analysis. Over 400 pollen grains and spores per sample were counted, with the maximum count reaching 798 grains (in one sample). Taxa percentage was calculated based on the total pollen and spore sum. CONISS was used for cluster analysis of pollen taxa. Pollen concentration and percentage diagrams were constructed using the *rioja* R package (Juggins, 2015).

To gain additional insights into the depositional environment and potential post-depositional processes, deteriorated pollen grains were analyzed separately (Hall, 1981; Chmura and Liu, 1990). Deteriorated pollen was differentiated in morphology as the grains are dark in colour with a damaged or corroded appearance. Several types of deteriorated pollen grains have been summarized,

TABLE 1 OSL ages of the samples collected from the LWM profile.

Sample	Depth (m)	U (ppm)	Th (ppm)	K (%)	Water content (%)	Equivalent dose (Gy)	Dose rate (Gy/ka)	Age (ka)	Grian size used for De estimation (μm)
LWM-2	2	4.56 ± 0.23	24.01 ± 0.95	2.42 ± 0.06	15 ± 10	4.83 ± 0.06	5.62 ± 0.37	0.86 ± 0.07	4~11
LWM-3.8	3.8	2.47 ± 0.06	12.18 ± 0.17	1.67 ± 0.02	10 ± 5	8.13 ± 0.66	2.94 ± 0.11	2.8 ± 0.3	63~90
LWM-4.2	4.2	1.98 ± 0.1	9.67 ± 0.43	1.69 ± 0.03	10 ± 5	7.24 ± 0.93	2.69 ± 0.11	2.7 ± 0.4	63~90
LWM-5.5	5.5	1.61 ± 0.04	7.43 ± 0.13	1.66 ± 0.01	10 ± 5	6.14 ± 0.29	2.43 ± 0.1	2.5 ± 0.2	63~90
LWM-6.15	6.15	2.02 ± 0.05	8.82 ± 0.12	1.74 ± 0.05	15 ± 5	6.5 ± 0.74	2.54 ± 0.1	2.6 ± 0.3	63~90
LWM-7.1	7.1	2.17 ± 0.04	10.48 ± 0.18	1.61 ± 0.03	15 ± 5	8.33 ± 0.45	3.07 ± 0.18	2.7 ± 0.2	4~11
LWM-8.5	8.5	1.87 ± 0.06	9.26 ± 0.17	1.58 ± 0.06	10 ± 5	17.78 ± 0.57	2.48 ± 0.11	7.2 ± 0.4	90~125

including corroded, degraded, mechanically damaged and obscured pollen grains (Lowe, 1982; Fernandes Pinto, 2012). These degraded grains are common in fluvial deposited pollen assemblages and are probably sourced during flood stages. Therefore, they are assumed to be an indicator of fluvial transport (Chmura and Liu, 1990; Wagstaff et al., 2013).

Grain size distributions of samples were determined using a Malvern Mastersizer 2000 with $(NaPO_3)_6$ as a dispersing agent after pre-treatment with HCl (10%) and H_2O_2 (30%) to remove secondary carbonates and organic matter. The measurement range of Mastersizer 2000 was 0.02–2,000 μm in grain diameter with a relative error of <1%.

4 Results

4.1 Stratigraphy and chronology

According to our previous research (Yang et al., 2023a; b), flood deposits in the profile have different sedimentary characteristics from lake deposits and sandy soils. In general, major flood deposits commonly contain an inverse-grading couple of fine-grained slackwater deposits (SWDs) and coarse-grained overbank deposits (ODs). The SWDs are red-brown clay with massive structures, and the ODs are a mixture of grey-yellow silt and sand with parallel laminations and ripples. The stratigraphy sequence from bottom to top was summarized as follows (Figure 2):

1) Unit I (900–825 cm) consists of coarse-grained sands with mud gravel at the bottom.
2) Unit II (825–755 cm) consists of grey-black silts of lacustrine deposits with dispersed shell fragments.
3) Unit III (755–358 cm) can be subdivided into three parts. The upper and lower parts are major flood deposits with ODs covering SWDs. The middle part, between 600–495 cm depth, contains several couplets of grey-yellow silt and brown-red silty clay with dual structures, supported by cycles of mean grain size.
4) Unit IV (358–190 cm) is brown sandy soil characterized by pores and redoximorphic features, interlining a thin flood layer between 280–330 cm depth.
5) Unit V (190–0 cm) contains flood deposits (190–20 cm) and modern soil (20–0 cm). Flood deposits are characterized by yellow silts and sands overlying red-brown silts. Modern soil is grey-brown clay with crumb structures.

Seven OSL dating results, ranging from 7.2 ± 0.4 ka to 0.86 ± 0.07 ka, follow the stratigraphic sequence (Table 1). At the bottom of Unit I, the OSL result is 7.2 ± 0.4 ka, and the radiocarbon dating result of lacustrine deposits in Unit II is 4,218–3,901 cal a BP. Five OSL results of flood deposits in Unit III are distributed around 2.7–2.5 ka, and one OSL result of the paleosol in Unit IV is 0.86± 0.07 ka. Considering the episodic deposition and hiatus in alluvial sediments, the Bayesian accumulation age-depth model was updated based on the lithological boundaries (Blaauw et al., 2018; Lombardi and Davis, 2022) (Figure 2). As a result, five sedimentary units were identified: before 7.3 ka (Unit I, 900–825 cm), 6.8–3.9 ka (Unit II, 825–755 cm); 3.2–2.2 ka (Unit III, 755–358 cm), 2.1–0.8 ka (Unit IV, 358–190 cm), and after 0.6 ka (Unit V, 190–0 cm). Both the sedimentary records and chronological results are mainly consistent with previous research sites (Yang et al., 2023b).

4.2 Palynology

A total of 66 pollen types were identified in 97 samples, including 20 arboreal pollen, 32 herb pollen, and 11 fern spores, with an average count of 414 grains per sample and an average concentration of 95 grains/g. Only taxa with a representation of >1% were used in Figure 3: *Pinus*, *Quercus*, Cereal, Amaranthaceae, *Artemisia*, *Polygonum*, Malvaceae, *Amethystea*, *Typha*, *Selaginella*, *Selaginella sinensis*, and Hymenophyllaceae. The LWM profile was divided into five pollen and three pollen-poor zones according to changes in the relative abundances and the CONISS cluster analysis result (Figure 3).

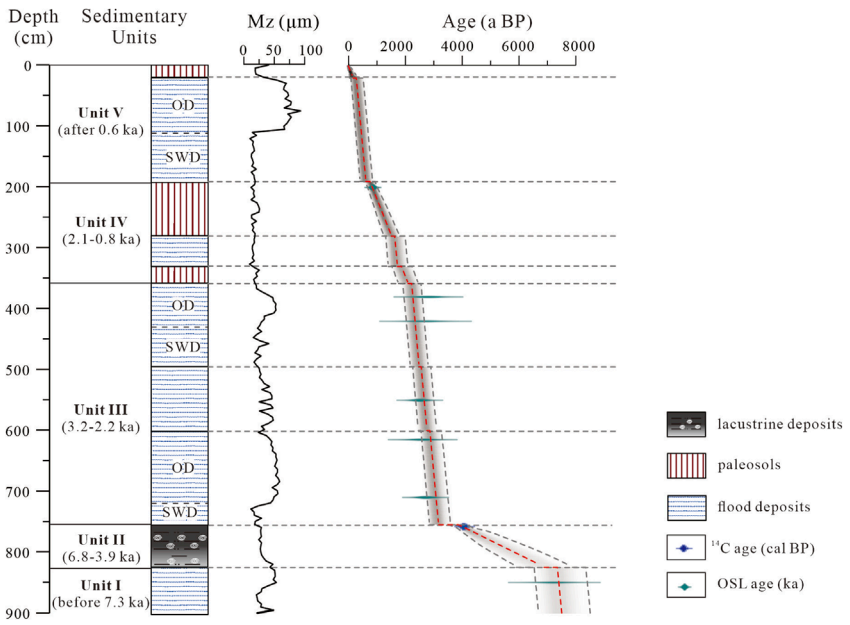

FIGURE 2
Sedimentary units, stratigraphy, dating results and Bayesian age-depth model based on OSL results of the LWM profile in the North China Plain. Gray dotted lines indicate 95% confidence intervals; the red dotted line shows the weighted mean age.

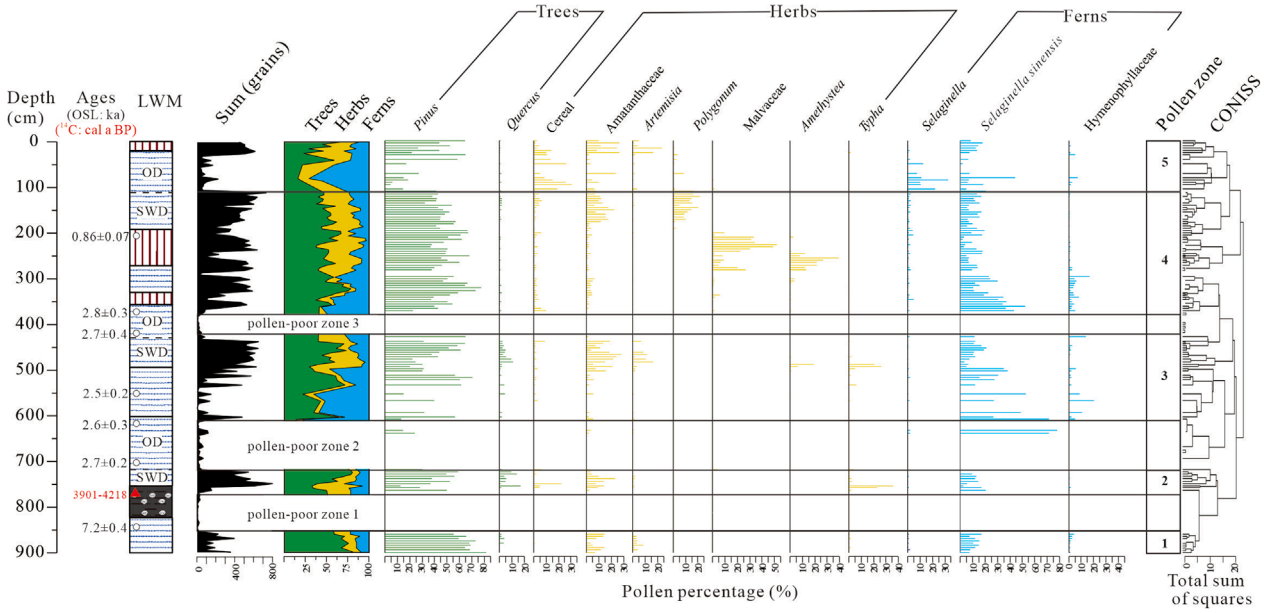

FIGURE 3
Stratigraphy and pollen percentage (%) from the LWM profile in the North China Plain. Legends are identical to Figure 2. The zone of most samples containing less than 100 grains of pollen and spores in total is marked as a "pollen-poor zone."

Pollen zone 1 (900–855 cm, before 7.3 ka): The average pollen concentration is 31 grains/g in six samples. The percentage of trees in this zone is the highest average in the profile (mean 70.4%), ranging from 58.8% to 82.4%. *Pinus*, the most dominant pollen type found throughout the LWM profile, also reaches its maximum (mean 65.7%). The herb pollen representation ranges from 8.2% to 19.0% (mean 14.8%), dominated by Amaranthaceae (mean 10.2%). The average percentage of ferns is 14.9% and is dominated by *S. sinensis* (mean 11.1%).

Pollen-poor zone 1 (855–765 cm, 7.4–4.3 ka): No analyzable samples were obtained.

Pollen zone 2 (765–720 cm, 4.3–3.1 ka): This zone consists of 9 samples. The mean pollen concentration increases to 77 grains/g, ranging from 25 to 146 grains/g. Arboreal pollen decreases to 55.8%

in this zone. *Pinus* has a representation of 42.6%, while *Quercus* increases to 6.4% in the layer of slackwater deposits with a maximum of 17.0%. Total herbaceous pollen percentages increase to 27.2%, mainly Cereal (0.4%–22.4%, mean value 4.1%), Amaranthaceae (2.6%–23.4%, mean value 9.8%), and *Typha* (0.5%–35.8%, mean value 7.6%). Ferns have similar characteristics to zone 1.

Pollen-poor zone 2 (720–610 cm, 3.1–2.9 ka): Only two samples have more than 100 grains per sample. These samples are characterized by a high percentage of ferns, dominated by *Selaginella sinensis*. *Selaginella sinensis* reaches its maximum value (78.0%) in this profile.

Pollen zone 3 (610–435 cm, 2.9–2.4 ka): This zone consists of 22 samples. The percentage of ferns (4.6%–77.9%, mean value 22.2%) decreases, especially *Selaginella sinensis* (3.6%–71.8%, mean value 23.0%) decrease rapidly. The herbaceous pollen increases from 5.3% to 62.0%, in which Amaranthaceae (mean value 10.9%), *Artemisia* (mean value 3.0%) and *Typha* (mean value 3.0%) increase significantly.

Pollen-poor zone 3 (435–365 cm, 2.4–2.2 ka): No samples meet the statistical data requirements.

Pollen zone 4 (365–110 cm, 2.2–0.5 ka): In this zone, 48 samples have high total grains (109–734 grains, mean value 438 grains). The pollen assemblages resemble those in zone 3, except that herbaceous pollens of *Polygonum* (mean value 3.8%) and Malvaceae (mean value 7.2%) start to appear. Arboreal pollen taxa dominated by *Pinus* (32.1%–77.8%, mean value 49.8%) increased to the mean value of 52.3%, while ferns dominated by *Selaginella sinensis* (1.8%–52.5%, mean value 15.1%) decreased to 20.9%.

Pollen zone 5 (110–0 cm, after 0.5 ka): This zone consists of 10 analyzable samples. The pollen grains decrease slightly to an average of 378 grains per sample (114–618 grains). This zone is distinguished by a substantial increase of herbaceous pollen, averaging 30.7%, ranging from 13.1% to 57.2%. Cereal (mean value 9.9%), Amaranthaceae (mean value 11.9%), and *Artemisia* (mean value 5.1%) all increase to the peak in the profile, while Malvaceae, *Amethystea* and *Typha* almost disappear from the record.

5 Discussion

5.1 Effects of sedimentation on pollen and spore distribution

It is widely accepted that pollen and spore distribution are closely related to the sedimentary environment (Brown, 1985; Xu et al., 1996; Zhu et al., 2002; Xu et al., 2016). In accordance with previous studies (Yang et al., 2023a; b), Unit II (825–755 cm) of lacustrine deposits and Unit IV (358–190 cm) dominated by sandy soils, represent relatively stable environments during flood-poor periods, while the other alluvial sediments get deposited in flood-prone periods. This interpretation is also supported by the regional stratigraphic comparison (Kidder et al., 2012; Storozum et al., 2018a; Yu et al., 2020). Pollen zones are consistent with the paleoenvironmental reconstruction results. For instance, *Typha*, an aquatic taxon, is mainly derived from lakes and wetlands in the NCP (Li et al., 2019). *Typha* appears in pollen zone 2, corresponding to the lacustrine deposit in Unit II. The percentage of herbs in pollen zone 4 increases to its highest value, corresponding to pedogenesis processes in Unit IV.

The pollen concentration is inversely correlated with grain size, suggesting hydrodynamics likely affect the distribution of types of sediment and pollen (Figure 4A). As Figure 4A shows, pollen concentration has the lowest value in coarse-grained deposits (mean size: 34.5 μm), but relatively high values in fine-grained slackwater deposits (mean size: 18.1 μm), and sandy soils (mean size: 19.1 μm). Fine-grained slackwater deposits were often accumulated in a relatively low-energy environments where the flood velocity was close to zero, and where pollen and spores were more likely to be enriched (Brush and Brush, 1972; Brown, 1985). For sandy soils, Pang et al. (2011) inferred that pollen assemblages from surface soil in the NCP have not only locally sourced plant types but also pollen components from regional mountains. Thus, local herbaceous taxa, including *Polygonum*, Malvaceae, and *Amethystea*, were mixed, and the total pollen content increased in paleosols (Liu et al., 2013; Liu et al., 2020). Unexpectedly, the low pollen concentration of lacustrine samples in the LWM profile (average 39.1 grains/g) was distinct from the results of regular lake deposits in the NCP, such as Baiyangdian and Ningjinpo (>100 grains/g) (Li et al., 2019). The result should be interpreted with caution, though, as our sample size was relatively small, based on only two valid samples.

Differences in pollen and spores existed between flood deposits and inter-flood deposits (Figure 4B). Previous research in the NCP argued that the percentage of arboreal pollen in flood deposits was higher than that in neighbouring paleosols (Liu et al., 2013;Liu et al., 2020). Nevertheless, the difference is not remarkable, and the relationship is even opposite in some cases (Liu et al., 2016). Moreover, the difference in pollen assemblages in multiphase flood deposits has not been discussed, as different types of paleoflood sediments are the most common scenario in the NCP (Kidder et al., 2012; Storozum et al., 2018a; b; Yu et al., 2020). In the LWM profile, the arboreal pollen percentage, dominated by *Pinus*, remains relatively high in different sediments. *Pinus* is regarded as an over-representative indicator because its pollen can be transported long-distances by airflows and rivers (Yang et al., 2021). In contrast, flood deposits have more ferns and fewer herbs than inter-flood deposits. Ferns dominated by *Selaginella sinensis* in overbank deposits showed higher average percentages (28.6%) than ferns in other deposits, despite its herbaceous pollen percentage being the lowest value (14.8%) overall. *Selaginella sinensis* mainly grows in alkaline soils in mountainous regions and was deposited with floods on plains, especially after regional forests were destroyed (Zhang and Kong, 1999; Tang et al., 2013). On the other hand, herbaceous pollen grains are more likely to accumulate in inter-flood deposits, because these pollen grains do not disperse over distance from their nearby parent plants (Yang et al., 2021).

5.2 Comparison of pollen results with paleoflood reconstructions

The complex relationship between pollen results and flood events was analyzed by comparison of pollen zones with paleoflood results. Six flooding periods have been reconstructed by sedimentary characteristics and confirmed by the grain size and chemical

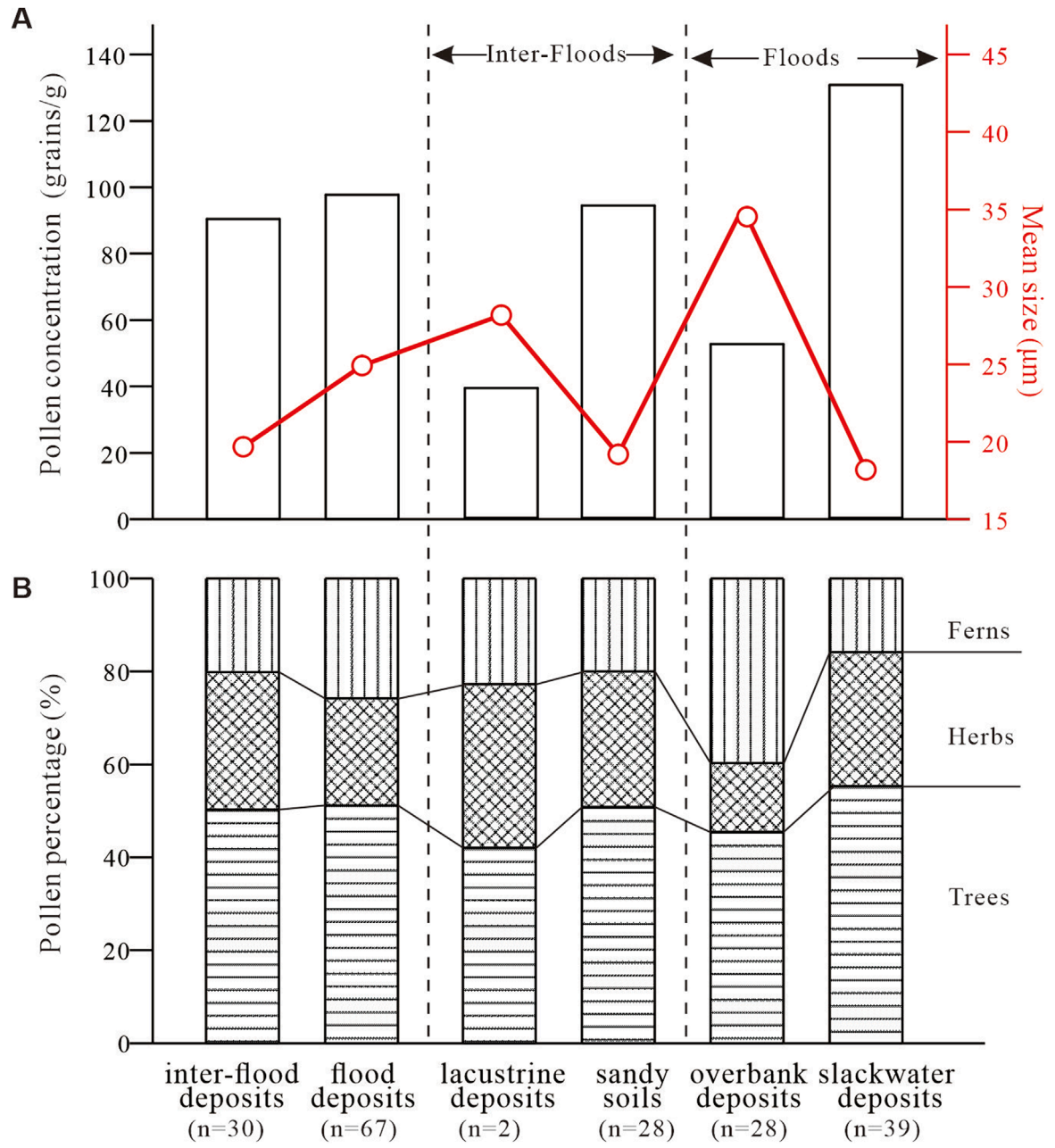

FIGURE 4
(A) The relationship between the total pollen concentration and mean grain size. **(B)** Comparison of pollen assemblage in different sediments of the LWM profile.

composition of sediments, including F1 of Unit I; F2, F3 and F4 of Unit III; F5 of Unit V; and F6 of Unit 5 (Yang et al., 2023b) (Figure 5). Both flooding Unit I (900–825 cm) and Unit III (755–360 cm) consist of pollen-poor zones at the top of flood periods. F6 of Unit V shows a similar trend with significantly low pollen concentration in pollen zone 5. However, our results suggest that pollen zones/subzones in the NCP cannot indicate flood events directly, which is inconsistent with previous research (Liu et al., 2020). The behavior of pollen grains and spores transported by river water is similar to that of sedimentary particles and they experience sorting effects (Brown, 1985; Moss et al., 2005). The protracted legacy of human activity, exacerbated by susceptible sedimentary environments in the NCP, can significantly complicate the interpretation of pollen and spores. Moreover, different sedimentary facies are closely interconnected in composition and formation, because inter-flooding sediments on floodplains are generally formed on pre-deposited alluvial deposits and are probably inundated by following overbank floods (Yang et al., 2023a; b). Thus, using pollen and spores as indicators for dividing sedimentary rhythms should be circumspect in an inconstant hydrodynamics environment.

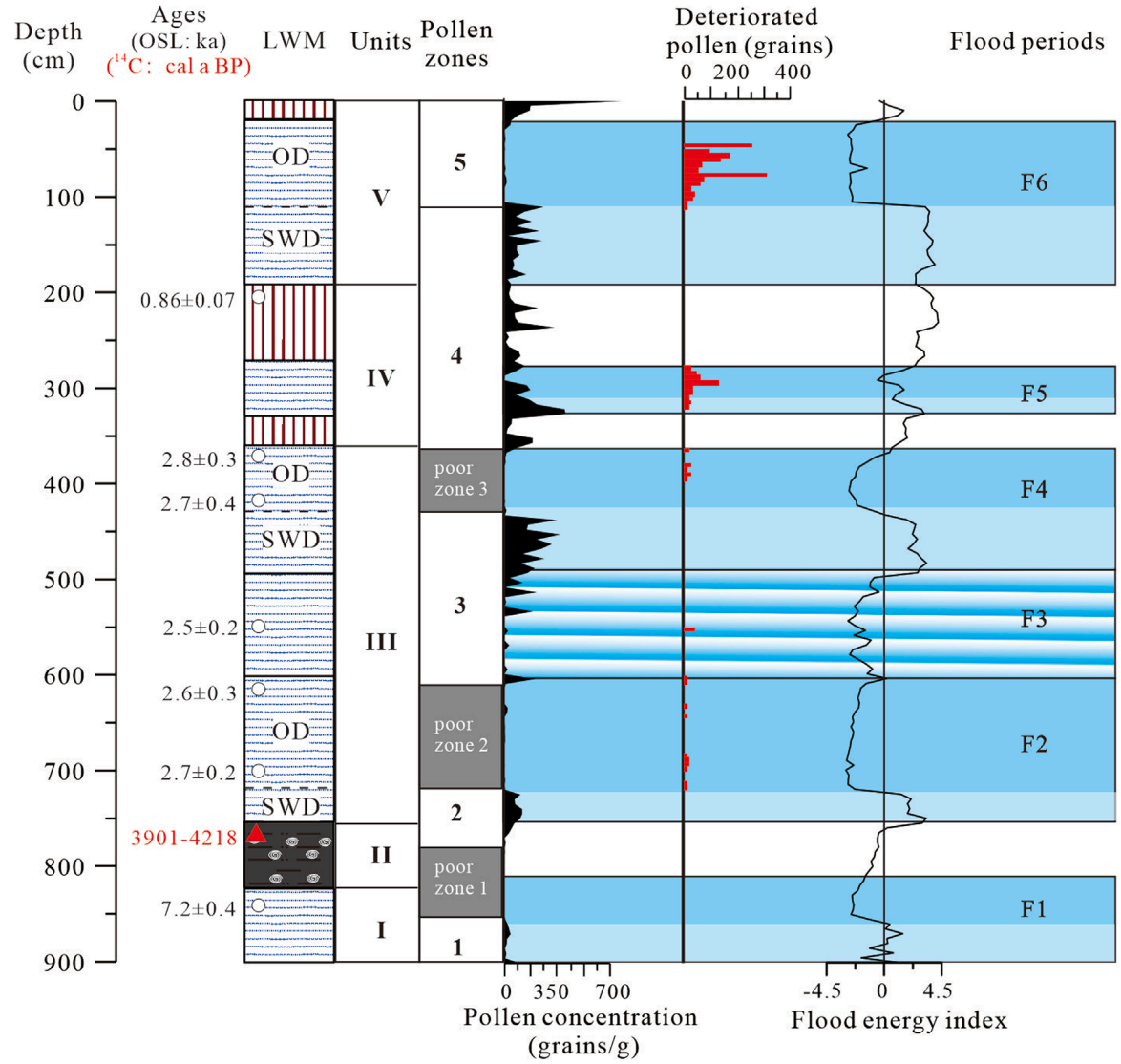

FIGURE 5
Pollen zones, pollen concentration, deteriorated pollen counts, flood energy index and flood periods of LWM profile.The paleoflood reconstruction refers to (Yang et al., 2023b). Legends are identical to Figure 2.

It is noteworthy that deteriorated pollen counts in the LWM profile are concentrated in coarse deposits (Figure 5). The mean 39 grains per sample of deteriorated pollen were detected in 46 samples of the LWM profile, with the maximum count reaching 311 grains at 85 cm depth (F6 in Figure 6). Furthermore, deteriorated pollen grains are consistent with the other flooding sedimentary units, including floods in Unit III (F2, F3 and F4 in Figure 6) and Unit IV (F5 in Figure 6). Deterioration of pollen, influenced by several factors, including mechanical damage, microbial activity, and geological processes (Lowe, 1982; Chmura and Eisma, 1995; Flantua et al., 2023). In alluvial environments, deteriorated and indeterminable pollen fossils are often related to overflows and floods, indicating an unstable depositional environment (e.g., Chmura and Liu, 1990). Hall (1981) indicated that higher frequencies of deteriorated grains corresponded with lower pollen concentration in a single stratigraphic column. Our findings produce similar conclusions to these studies. This strong consistency between deteriorated pollen and flood periods probably confirms its indicative of strong hydrological conditions at the flood-peak period.

5.3 Implications for pollen-based anthropogenic impacts

Representative non-arboreal pollen taxa in the NCP suggests increased anthropogenic activity since ca. 4.0 ka. No obvious palynological evidence of anthropogenic impacts is detected in pollen zone 1. However, herbaceous pollen percentages increase rapidly and cereal pollen starts to appear at the onset of pollen zone 2. These characteristics are closely related to human activities (Li et al., 2008; Cao et al., 2010), which probably reveal that anthropogenic forest disturbance and cereal cultivation have

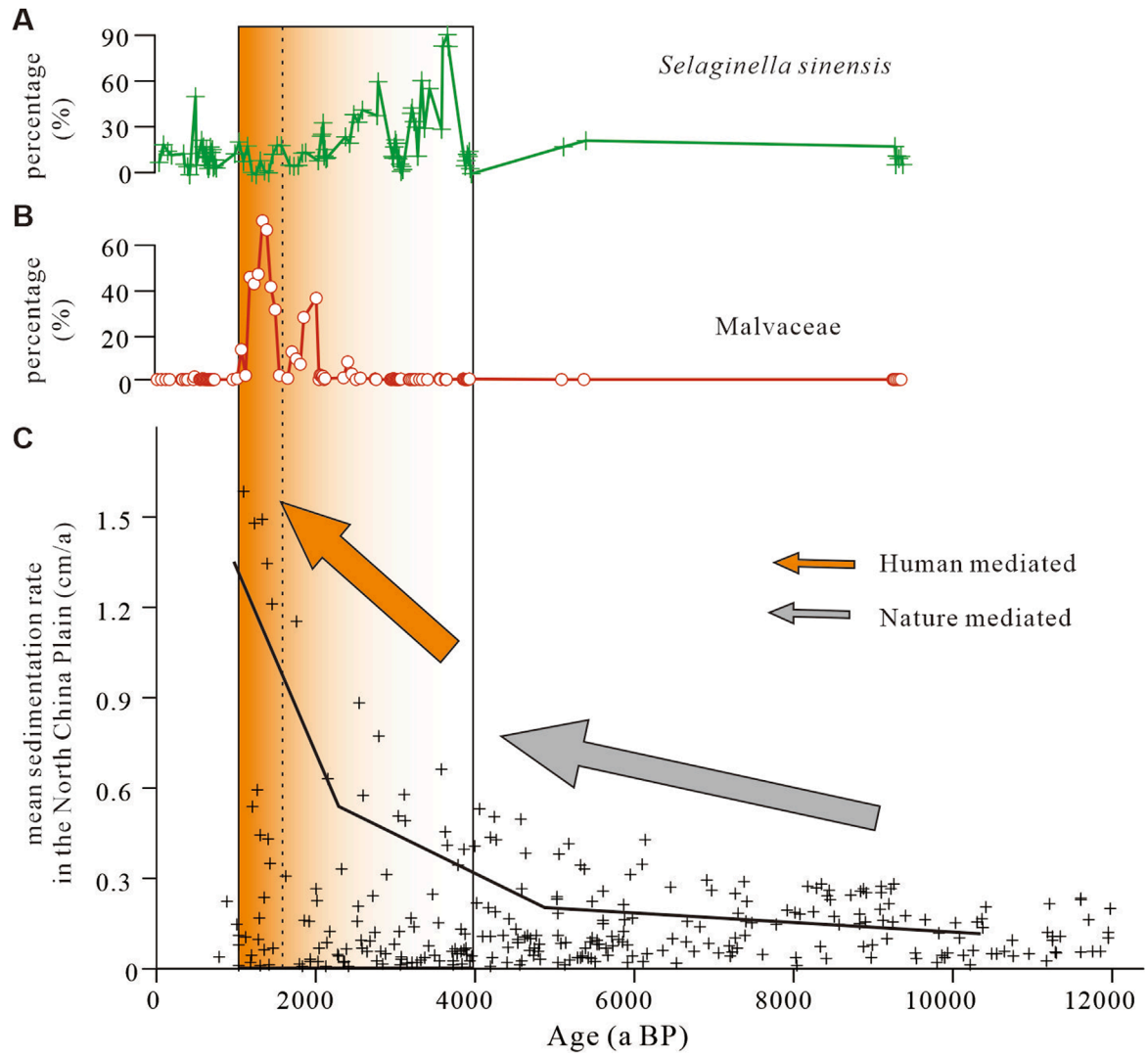

FIGURE 6
The variation of *Selaginella sinensis* **(A)** and Malvaceae **(B)** in the LWM profile. **(C)** The average sedimentation rates in the North China Plain since the Holocene (modified from (Xu, 1998; Shi et al., 2010)).

occurred since ca. 4.3 ka. Furthermore, *Selaginella sinensis* spores aggregated at 640–610 cm and increased to the highest percentage of 77.98% (ca. 2.9 ka) (Figures 3, 6A). *Selaginella sinensis* is an indicator of deforestation by intense human activities in uplands, which is an adopted practice in the NCP (Zhang et al., 2007; Cao et al., 2010; Xu et al., 2010). Based on the above pollen analysis, it can thus be concluded that human activity has been amplified around 4.0–3.0 ka.

Local agriculture in the Daming area is intensified in pollen zone 4, which is inferred from the significant increase of Malvaceae. A strong correlation between cotton and Malvaceae has been observed in the field of botanical research (Wang and Li, 1994). Malvaceae increased to its peak value between 285–215 cm (Figures 3, 6B), suggesting that widespread cotton cultivation probably appeared since ca. 1.6–1.0 ka. In addition, agricultural history in the Hebei province also supports the initial period of cotton planting from the Tang Dynasty (ca. 1.4–1.1 ka) (Cui et al., 2019). Therefore, it is safe to infer that this stage represents intensified agricultural activity.

Human impacts inferred from the pollen record are consistent with regional research, which further confirms that large-scale human activities in the study area have gradually accelerated since the late Holocene. The average sedimentation rate within the NCP is characterized by rapid increases around 5.0 ka and 2.3 ka (Figure 6C), which are theorized to be due to growing human influence (Xu, 1998; Shi et al., 2002). This sediment pattern is supported by the concentrated percentages of *Selaginella sinensis* (Figure 6A) and Malvaceae (Figure 6B), which are indicative of deforestation and agricultural expansion, respectively. Furthermore, pollen assemblages from archaeological sites in the piedmont region of the Taihang Mountains suggested that the growing human footprint and impact of urban settlement was accelerated, especially large-scale deforestation occurring after ca. 3.4 ka (Cao et al., 2010; Ren et al., 2019). Nearby geoarchaeological research in the study

area also uncovered that humans began to influence alluvial deposits around 4.0 ka, and agricultural production intensified during the Tang-Song Dynasty (ca. 1.4–0.7 ka) (Storozum et al., 2018a). In conclusion, the palynological findings align with regional research, providing compelling evidence for the progressive intensification of human activities within the NCP.

In this paper, there may be two major limitations that could be addressed in future research. Firstly, the valid samples are relatively limited, and therefore, the results of the study may not be representative of the entire region or period. Future studies should focus on increasing pollen data in fluvial-lacustrine sediments to improve the statistical power of the results (Flantua et al., 2023). Secondly, the possibility of redeposited pollen grains should be considered. The deteriorated pollen in the profile, dominated by *Pinus* and Hymenophyllaceae, cannot be confirmed to be reworked pollen at present because the separation of reworked Holocene pollen from recent pollen is next to impossible without other evidence (Stanley, 1965).

6 Conclusion

(1) In the LWM profile, pollen concentration shows a strong negative correlation with grain size, and pollen assemblages correspond to different sedimentary facies representing flooding and inter-flooding periods. Compared with arboreal pollen, dominated by over-representative *Pinus*, the content of herbaceous pollen and fern spores shows a more significant difference between flood deposits and inter-flood deposits.

(2) Flooding units are characterized by pollen-poor zones and deteriorated pollen grains in the overlying coarse-grained deposits at the flood-peak stage. The impressive floods are predominantly responsible for the complexity of pollen assemblages seen here.

(3) Rapid shrinkage of arboreal pollen and increases in pollen indicative of human activity (e.g., Cereal and Malvaceae) demonstrates the intense human impact since the late Holocene. Specifically, significant forest destruction and anthropogenic soil erosion in piedmont areas impacted alluvial pollen after ca. 2.9 ka, and large-scale agricultural activities were intensified after ca. 1.6 ka. This research highlights past flood events and human activity as the two main factors controlling the landform of the North China Plain.

Data availability statement

The original contributions presented in the study are included in the article/Supplementary Material, further inquiries can be directed to the corresponding authors.

Author contributions

JY: Conceptualization, Data curation, Formal Analysis, Funding acquisition, Investigation, Methodology, Project administration, Software, Visualization, Writing–original draft, Writing–review and editing. LL: Funding acquisition, Methodology, Supervision, Writing–review and editing. HR: Methodology, Writing–original draft, Writing–review and editing. ZL: Data curation, Investigation, Methodology, Writing–original draft. LS: Funding acquisition, Investigation, Methodology, Writing–original draft. PZ: Investigation, Visualization, Writing–original draft.

Funding

The author(s) declare financial support was received for the research, authorship, and/or publication of this article. This work was supported by the Basic Research Program of the Chinese Academy of Geological Sciences (No. YK202308), the National Natural Science Foundation of China (Nos. 41807428 and 42177428), the Hebei Natural Science Foundation (Nos. D2020504008 and D2020504018), and the China Geological Survey (No. DD20221929).

Acknowledgments

We sincerely thank Prof. Mark Macklin, Dr. Kristen K. Beck, Gertruda Zieniute, and Josephine Westlake at the University of Lincoln, United Kingdom, for their comments on an early draft of this paper. The authors are grateful to Dr. Xin Mao and Shuxian Fan for their help with pollen analysis. Reviewers are acknowledged for their supportive comments.

Conflict of interest

The authors declare that the research was conducted in the absence of any commercial or financial relationships that could be construed as a potential conflict of interest.

Publisher's note

All claims expressed in this article are solely those of the authors and do not necessarily represent those of their affiliated organizations, or those of the publisher, the editors and the reviewers. Any product that may be evaluated in this article, or claim that may be made by its manufacturer, is not guaranteed or endorsed by the publisher.

References

Alexandrovskiy, A. L., Ershova, E. G., and Krenke, N. A. (2016). Buried late-holocene luvisols of the oka and moskva river floodplains and their anthropogenic evolution according to soil and pollen data. *Quat. Int.* 418, 37–48. doi:10.1016/j.quaint.2015.12.094

Bai, X., Wu, Z., Zhang, Y., Lu, G., Liu, C., Ren, X., et al. (2015). Survey of the ancient city of daming palace, hebei province. *Cult. Relics Age* 5, 27–34. (In Chinese).

Blaauw, M., Christen, J. A., Bennett, K. D., and Reimer, P. J. (2018). Double the dates and go for bayes — impacts of model choice, dating density and quality on chronologies. *Quat. Sci. Rev.* 188, 58–66. doi:10.1016/j.quascirev.2018.03.032

Brown, A. G. (1985). The potential use of pollen in the identification of suspended sediment sources. *Earth Surf. Process. Landf.* 10 (1), 27–32. doi:10.1002/esp.3290100106

Brown, A. G., Carpenter, R. G., and Walling, D. E. (2008). Monitoring the fluvial palynomorph load in a lowland temperate catchment and its relationship to suspended sediment and discharge. *Hydrobiologia* 607 (1), 27–40. doi:10.1007/s10750-008-9364-6

Brush, G. S., and Brush, L. M. (1972). Transport of pollen in a sediment-laden channel:a laboratory study. *Am. J. Sci.* 4 (272), 359–381. doi:10.2475/ajs.272.4.359

Cao, X., Xu, Q., Jing, Z., Tang, J., Li, Y., and Tian, F. (2010). Holocene climate change and human impacts implied from the pollen records in anyang, central China. *Quat. Int.* 227 (1), 3–9. doi:10.1016/j.quaint.2010.03.019

Chen, Y. (2019). Flood dynamics of the lower yellow river over the last 3000 years: characteristics and implications for geoarchaeology. *Quat. Int.* 521, 147–157. doi:10.1016/j.quaint.2019.05.040

Chen, Y., Chen, S., Liu, J., Yao, M., Sun, W., and Zhang, Q. (2013). Environmental evolution and hydrodynamic process of dongping lake in shandong province, China, over the past 150 years. *Environ. Earth Sci.* 68 (1), 69–75. doi:10.1007/s12665-012-1716-x

Chen, Y., Syvitski, J. P. M., Gao, S., Overeem, I., and Kettner, A. J. (2012). Socio-economic impacts on flooding: a 4000-year history of the yellow river, China. *Ambio* 41 (7), 682–698. doi:10.1007/s13280-012-0290-5

Chevalier, M., Davis, B. A. S., Heiri, O., Seppä, H., Chase, B. M., Gajewski, K., et al. (2020). Pollen-based climate reconstruction techniques for late quaternary studies. *Earth-Sci. Rev.* 210, 103384. doi:10.1016/j.earscirev.2020.103384

Chmura, G. L., and Eisma, D. (1995). A palynological study of surface and suspended sediments on a tidal flat; Implications for pollen transport and deposition in coastal waters. *Mar. Geol.* 128 (3-4), 183–200. doi:10.1016/0025-3227(95)00096-H

Chmura, G. L., and Liu, K. (1990). Pollen in the lower Mississippi river. *Rev. Palaeobot. Palynol.* 64 (1), 253–261. doi:10.1016/0034-6667(90)90140-E

Cui, R., Tian, H., and Zhou, Y. (2019). The initial period of cotton planting in hebei province. *J. Agric.* 4 (9), 92–94. (In Chinese with English abstract).

Daming County Local Gazetteers Compilation Committee (1994). *Natural disaster daming county local Gazetteers (99-112)*. Beijing: Xinhua Publishing House. (Reprinted.

Ding, W., Pang, R., Xu, Q., Li, Y., and Cao, X. (2011). Surface pollen assemblages as indicators of human impact in the warm temperate hilly areas of eastern China. *Chin. Sci. Bull.* 56 (10), 996–1004. doi:10.1007/s11434-011-4350-1

Durcan, J. A., King, G. E., and Duller, G. A. T. (2015). Drac: dose rate and age calculator for trapped charge dating. *Quat. Geochronol.* 28, 54–61. doi:10.1016/j.quageo.2015.03.012

Faegri, K., and Iversen, J. (1964). *Textbook of pollen analysis*. Copenhagen: Munksggard.

Fan, S., Liu, H., Xu, J., Zheng, H., Zhao, H., Bi, Z., et al. (2009). Palaeovegetation and environmental evolution in hengshui district of hebei province since 3.50 ma bp. *Geoscience* 1 (23), 75–81. (In Chinese with English abstract).

Fernandes Pinto, C. (2012). *Palynology as a tool in bathymetry: IntechOpen*. (Reprinted.

Flantua, S. G. A., Mottl, O., Felde, V. A., Bhatta, K. P., Birks, H. H., Grytnes, J. A., et al. (2023). A guide to the processing and standardization of global palaeoecological data for large-scale syntheses using fossil pollen. *Glob. Ecol. Biogeogr.* 32 (8), 1377–1394. doi:10.1111/geb.13693

Hall, S. A. (1981). Deteriorated pollen grains and the interpretation of quaternary pollen diagrams. *Rev. Palaeobot. Palynol.* 32 (2-3), 193–206. doi:10.1016/0034-6667(81)90003-8

Juggins, S. (2015). *Rioja: analysis of quaternary science data*.

Kidder, T. R., Liu, H., and Li, M. (2012). Sanyangzhuang: early farming and a han settlement preserved beneath yellow river flood deposits. *Antiquity* 86 (331), 30–47. doi:10.1017/S0003598X0006244X

Kumar, S., Luo, C., Rahman, A., Thilakanayaka, V., Khan, M. H. R., Liu, J., et al. (2019). Modern alluvial pollen distribution in ganges–brahmaputra–meghna (gbm) floodplain and its paleoenvironmental significance. *Rev. Palaeobot. Palynol.* 267, 1–16. doi:10.1016/j.revpalbo.2019.04.008

Li, K., Gu, Y., and Liu, H. (2016). Holocene climate changes derived from spore-pollen records and neolithic culture succession in northern henan plain. *J. Jilin Univ.* 46 (5), 1449–1457. (In Chinese with English abstract).

Li, M., Zhang, S., Xu, Q., Xiao, J., and Wen, R. (2019). Spatial patterns of vegetation and climate in the north China plain during the last glacial maximum and holocene climatic optimum. *Sci. China Earth Sci.* 62 (8), 1279–1287. doi:10.1007/s11430-018-9264-2

Li, Y., Zhou, L., and Cui, H. (2008). Pollen indicators of human activity. *Sci. Bull.* 53 (9), 1281–1293. doi:10.1007/s11434-008-0181-0

Liu, D., Ma, J., Gu, L., and Chen, Y. (2016). The middle and late holocene pollen record from the yellow river flooding sedimentary sequence in the western suburbs of kaifeng city, China. *Acta Geogr. Sin.* 71 (5), 852–863. (In Chinese with English abstract).

Liu, D., Ma, J., Wu, P., and Pan, Y. (2020). A new indicator for dividing sedimentary rhythms in alluvial deposits: a pollen-based method. *Catena* 189, 104500. doi:10.1016/j.catena.2020.104500

Liu, Y., Xu, Q., Li, M., Zhang, S., Liu, H., Zhu, J., et al. (2013). Holocene pollen record of the sanyangzhuang site in neihuang county,henan province. *Quat. Sci.* 33 (3), 536–544. (In Chinese with English abstract).

Lombardi, R., and Davis, M. A. L. (2022). Incorporating alluvial hydrogeomorphic complexities into paleoflood hydrology, magnitude estimation and flood frequency analysis, Tennessee river, Alabama. *J. Hydrol.* 612, 128085. doi:10.1016/j.jhydrol.2022.128085

Lombardo, U. (2016). Alluvial plain dynamics in the southern amazonian foreland basin. *Earth Syst. Dynam.* 7 (2), 453–467. doi:10.5194/esd-7-453-2016

Lowe, J. J. (1982). Three flandrian pollen profiles from the teith valley, perthshire, scotland; Ii. Analysis of deteriorated pollen. *New Phytologist* 90 (2), 371–385. doi:10.1111/j.1469-8137.1982.tb03268.x

Lv, K., Shi, G., Zhang, H., Zhang, J., Li, Q., and Zhang, P. (2022). Quaternary palynological records and climatic signifiance of s9 borehole in sanhe city of hebei plain. *Geol. Surv. China* 9 (1), 64–72. (In Chinese with English abstract).

Moss, P. T., Kershaw, A. P., and Grindrod, J. (2005). Pollen transport and deposition in riverine and marine environments within the humid tropics of northeastern Australia. *Rev. Palaeobot. Palynol.* 134 (1-2), 55–69. doi:10.1016/j.revpalbo.2004.11.003

Murray, A. S., and Wintle, A. G. (2000). Luminescence dating of quartz using an improved single-aliquot regenerative-dose protocol. *Radiat. Meas.* 32 (1), 57–73. doi:10.1016/S1350-4487(99)00253-X

Pang, R., Xu, Q., Ding, W., and Zhang, S. (2011). Pollen assemblages of cultivated vegetation in central and southern hebei province. *J. Geogr. Sci.* 21 (3), 549–560. doi:10.1007/s11442-011-0863-4

Reimer, P. J., Austin, W. E. N., Bard, E., Bayliss, A., Blackwell, P. G., Bronk Ramsey, C., et al. (2020). The intcal20 northern hemisphere radiocarbon age calibration curve (0-55 cal kbp). *Radiocarbon* 62 (4), 725–757. doi:10.1017/RDC.2020.41

Ren, X., Mo, D., Storozum, M., Lemoine, X., Yu, Y., Gu, W., et al. (2019). Early urban impact on vegetation dynamics: palaeoecological reconstruction from pollen records at the dongzhao site, henan province, China. *Quat. Int.* 521, 66–74. doi:10.1016/j.quaint.2019.07.012

Ricker, M. C., Stolt, M. H., and Zavada, M. S. (2019). Pollen preservation in alluvial soils; Implications for paleoecology and land use studies. *Soil Sci. Soc. Am. J.* 83 (5), 1595–1600. doi:10.2136/sssaj2019.01.0025

Shi, C., Dian, Z., and You, L. (2002). Changes in sediment yield of the yellow river basin of China during the holocene. *Geomorphology* 46 (3–4), 267–283. doi:10.1016/S0169-555X(02)00080-6

Shi, C., Zhang, L., Xu, J., and Guo, L. (2010). Sediment load and storage in the lower yellow river during the late holocene. *Geogr. Ann. Ser. a, Phys. Geogr.* 92 (3), 297–309. doi:10.1111/j.1468-0459.2010.00396.x

Shi, J., Liu, C., Dong, H., Yan, Z., Wang, Y., Liu, X., et al. (2014). Stability assessment and risk analysis of aboveground river in lower yellow river. *J. Groundw. Sci. Eng.* 2 (4), 1–18. doi:10.26599/JGSE.2014.9280037

Solomon, A. M., Blasing, T. J., and Solomon, J. A. (1982). Interpretation of floodplain pollen in alluvial sediments from an arid region. *Quat. Res.* 18 (1), 52–71. doi:10.1016/0033-5894(82)90021-7

Stanley, E. A. (1965). Use of reworked pollen and spores for determining the pleistocene-recent and the intra-pleistocene boundaries. *Nature* 206 (4981), 289–291. doi:10.1038/206289a0

Storozum, M., Liu, H., Qin, Z., Ming, K., Fu, K., Wang, H., et al. (2018b). Early evidence of irrigation technology in the north China plain: geoarchaeological investigations at the anshang site, neihuang county, henan province, China. *Geoarchaeology* 33 (2), 143–161. doi:10.1002/gea.21634

Storozum, M., Qin, Z., Ren, X., Li, H., Cui, Y., Fu, K., et al. (2018a). The collapse of the north song dynasty and the ad 1048–1128 yellow river floods: geoarchaeological evidence from northern henan province, China. *Holocene* 28 (11), 1759–1770. doi:10.1177/0959683618788682

Tang, L., Mao, L., Lü, X., Ma, Q., Zhou, Z., Yang, C., et al. (2013). Palaeoecological and palaeoenvironmental significance of some important spores and micro-algae in quaternary deposits. *Chin. Sci. Bull.* 58 (25), 3125–3139. doi:10.1007/s11434-013-5747-9

Tong, G., Ke, M., and Yu, S. (1983). Quaternary sporo-pollen assemblages in hebei plain, China and their geological significance. *Mar. Geol. Quat. Geol.* (4), 91–103. (In Chinese with English abstract).

Wagstaff, B. E., Gallagher, S. J., Norvick, M. S., Cantrill, D. J., and Wallace, M. W. (2013). High latitude albian climate variability: palynological evidence for long-term drying in a greenhouse world. *Palaeogeogr. Palaeoclimatol. Palaeoecol.* 386, 501–511. doi:10.1016/j.palaeo.2013.06.018

Wang, F. X., Chien, N. F., Zhang, Y. L., and Yang, H. Q. (1995). *Pollen flora of China (in Chinese)*. 2nded. Beijing: Science Press.

Wang, R., and Li, X. (1994). Morpholgical relation among direction of petals' orderm seminal leaves and leaf rank in cotton and some plants else of malvaceae and other families. *Acta Agron. Sin.* (04), 489–495.

Wintle, A. G., and Murray, A. S. (2006). A review of quartz optically stimulated luminescence characteristics and their relevance in single-aliquot regeneration dating protocols. *Radiat. Meas.* 41 (4), 369–391. doi:10.1016/j.radmeas.2005.11.001

Wohl, E. (2021). An integrative conceptualization of floodplain storage. *Rev. Geophys.* 59 (2), e2020RG000724. doi:10.1029/2020RG000724

Xu, J. (1998). Naturally and anthropogenically accelerated sedimentation in the lower yellow river, China, over the past 13,000 years. *Geogr. Ann. Ser. a, Phys. Geogr.* 80 (1), 67–78. doi:10.1111/1468-0459.00027

Xu, Q., Cao, X., Wang, X., Li, Y., and Jing, Z. (2010). Generation of yinxu culture: environmental background and impacts of human activities. *Quat. Sci.* 30 (2), 273–286. (In Chinese with English abstract).

Xu, Q., Yang, X., Wu, C., Meng, L., and Wang, Z. (1996). Alluvial pollen on the north China plain. *Quat. Res.* 46 (3), 270–280. doi:10.1006/qres.1996.0066

Xu, Q., Zhang, S., Gaillard, M., Li, M., Cao, X., Tian, F., et al. (2016). Studies of modern pollen assemblages for pollen dispersal-deposition- preservation process understanding and for pollen-based reconstructions of past vegetation, climate, and human impact: a review based on case studies in China. *Quat. Sci. Rev.* 149, 151–166. doi:10.1016/j.quascirev.2016.07.017

Yang, J., Liu, L., Zhao, H., Liu, Z., Song, L., Zhang, P., et al. (2023a). Late holocene sedimentary records along the abandoned channel areas of the yellow river and their response to flood hazards. *Geol. China* 4 (50), 1004–1015. doi:10.12029/gc20220323001

Yang, J., Liu, Z., Yin, J., Tang, L., Zhao, H., Song, L., et al. (2023b). Paleoflood reconstruction in the lower yellow river floodplain (China) based on sediment grain size and chemical composition. *Water* 15 (24), 4268. doi:10.3390/w15244268

Yang, S., Li, J., Ye, S., Mackenzie, L., Yuan, H., He, L., et al. (2021). Pollen distribution and transportation patterns in surface sediments of liaodong bay, China. *Sci. Total Environ.* 771, 144883. doi:10.1016/j.scitotenv.2020.144883

Yang, S., Song, B., Ye, S., Laws, E. A., He, L., Li, J., et al. (2019). Large-scale pollen distribution in marine surface sediments from the bohai sea, China: insights into pollen provenance, transport, deposition, and coastal-shelf paleoenvironment. *Prog. Oceanogr.* 178, 102183. doi:10.1016/j.pocean.2019.102183

Yu, L., Liu, H., Wan, F., Hu, Z., Luo, H., and Zhang, X. (2021). Geochemical records of the sediments and their significance in dongping lake area, the lower reach of yellow river, north China. *J. Groundw. Sci. Eng.* 9 (2), 140–151. doi:10.19637/j.cnki.2305-7068.2021.02.006

Yu, S., Hou, Z., Chen, X., Wang, Y., Song, Y., Gao, M., et al. (2020). Extreme flooding of the lower yellow river near the northgrippian-meghalayan boundary: evidence from the shilipu archaeological site in southwestern shandong province, China. *Geomorphology* 350, 106878. doi:10.1016/j.geomorph.2019.106878

Zhang, J., and Kong, Z. (1999). Significance on ecological indication of selaginella sinensis in reconstructing past environment. *Acta Bot. Boreali-Occidentalia Sin.* 19, 530–537. (In Chinese with English abstract).

Zhang, Z., Xu, Q., Li, Y., Yang, X., Jin, Z., and Tang, J. (2007). Environmental changes of the yin ruins area based on pollen analysis. *Quat. Sci.* 27 (3), 461–468. (In Chinese with English abstract).

Zhu, Y., Chen, F., and Madsen, D. (2002). The environmental signal of an early holocene pollen record from the shiyang river basin lake sediments, nw China. *Chin. Sci. Bull.* 47 (4), 267–273. doi:10.1360/02tb9065